Direct synthesis of amides from amines using mesoporous Mn-SBA-12 and Mn-SBA-16 catalysts

ARTICLE *in* CATALYSIS COMMUNICATIONS · JULY 2013

Impact Factor: 3.7 · DOI: 10.1016/j.catcom.2013.03.020

3 AUTHORS, INCLUDING:

Dr. Anuj Kumar
Indian Institute of Technology Ropar
7 PUBLICATIONS **52** CITATIONS
SEE PROFILE

Devadutta Nepak
CSIR - National Chemical Laboratory, Pune
2 PUBLICATIONS **6** CITATIONS
SEE PROFILE

Catalysis Communications 37 (2013) 36–40

Contents lists available at SciVerse ScienceDirect

Catalysis Communications

journal homepage: www.elsevier.com/locate/catcom

Short Communication

Direct synthesis of amides from amines using mesoporous Mn-SBA-12 and Mn-SBA-16 catalysts

Anuj Kumar, Devadutta Nepak, Darbha Srinivas *

Catalysis Division, CSIR-National Chemical Laboratory, Pune, 411008, India

ARTICLE INFO

Article history:
Received 21 February 2013
Received in revised form 18 March 2013
Accepted 20 March 2013
Available online 27 March 2013

Keywords:
Manganese incorporated SBA-12 and SBA-16
Amide synthesis
Aerial oxidation
Benzyl amine
Mesoporous Mn-silica catalyst

ABSTRACT

Manganese incorporated SBA-12 and SBA-16 catalyze the tandem reaction of aliphatic primary amine, aerial oxygen and ammonia solution at moderate conditions producing amide in yields as high as 50 mol%. The Mn-SBA-12 and Mn-SBA-16 catalysts with Si/Mn output molar ratio in the range 230 to 748 were prepared by the direct hydrothermal synthesis method and characterized. Weak acidity and Mn in +3 oxidation state are the key factors enable the synthesis of product amide in high yields.

1. Introduction

Amides are valuable chemicals. Methacrylamide and caprolactum are two industrially important amides used in polymer manufacturing [1]. Amides find application also in the treatment of HIV and cardiovascular diseases, hypertension and high blood pressure [2]. Conventionally, they are prepared by reacting amines with acid chloride or anhydride [3]. This method is non-ecofriendly as equimolar amount of acid is generated as waste. Several elegant approaches have been reported which include the synthesis from primary alcohols and amines using pincer-type ruthenium complex [4], from various aldoximes in water over rhodium hydroxide on alumina [5] and by direct oxygenation of primary amines in presence of water using ruthenium hydroxide supported on alumina catalysts [6]. All these methods use expensive metal catalysts. Development of a greener approach which doesn't generate waste and uses cheaper metal catalysts is desired. Wang et al. [7] reported that manganese oxide octahedral molecular sieves catalyze the direct conversion of primary amines to amides. We report here, for the first time, the application of manganese incorporated mesoporous silica (Mn-SBA-12 and Mn-SBA-16) catalysts for preparing amides from primary amines by direct reaction with aerial oxygen and ammonia solution.

2. Experimental

2.1. Catalyst preparation and characterization

Mn-containing SBA-12 and SBA-16 were prepared by direct hydrothermal synthesis method using Brij76 and Pluronic F127 structure directing agents and 0.1 M and 2 M HCl solutions, respectively. Tetraethyl orthosilicate and $Mn(NO_3)_2 \cdot 4H_2O$ were used as Si and Mn sources, respectively. Detailed synthesis and characterization procedures are provided in Supplementary data, S1.

2.2. Reaction procedure

Benzylamine (5 mmol), 1,4-dioxane (15 mL), 25 wt.% aqueous ammonia (1 mL) and catalyst (0.2 g) were charged into a 100 mL stainless-steel reactor (Paar 4875 power controller and 4871 process controller) which was then pressurized with air (6–10 bar). Temperature of the reactor was raised to 373–423 K and the reaction was conducted for a desired period of time (2–10 h). After the completion of reaction, the reactor was brought to 298 K and the air remained was vented out. The catalyst was separated by filtration and the liquid product was analyzed by gas chromatography and identified by GC–MS.

3. Results and discussion

3.1. Structural and textural characterization

Small-angle X-ray diffraction (XRD) patterns of Mn-SBA-12 showed a main peak at 1.67° due to (002) reflection and two less

* Corresponding author. Tel.: +91 20 2590 2018; fax: +91 20 2590 2633.
E-mail address: d.srinivas@ncl.res.in (D. Srinivas).

1566-7367/$ – see front matter © 2013 Elsevier B.V. All rights reserved.
http://dx.doi.org/10.1016/j.catcom.2013.03.020

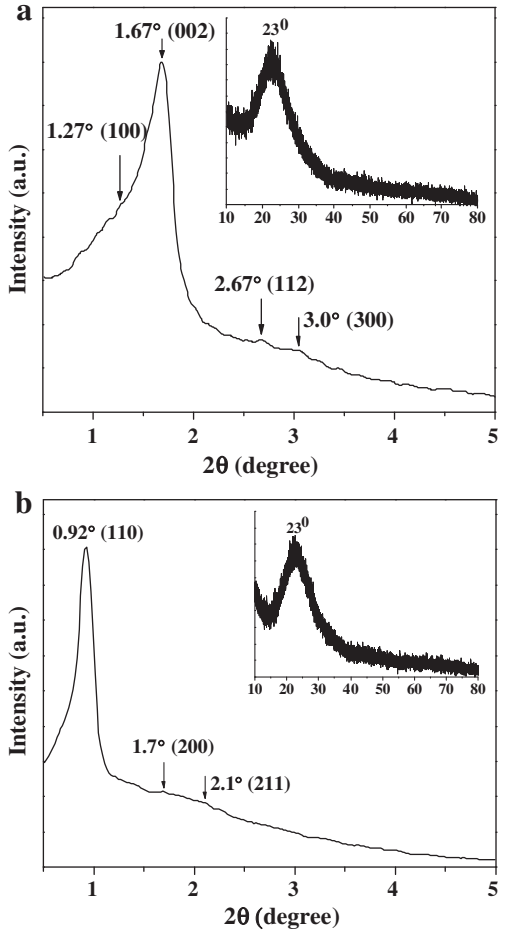

Fig. 1. Small- and wide-angle (inset) XRD profiles of (a) Mn-SBA-12 (Si/Mn = 230) and (b) Mn-SBA-16 (Si/Mn = 278).

resolved peaks at 2.67° and 3.0° corresponding to (112) and (300) reflections, respectively (Fig. 1). A weak shoulder to the main peak arising from (100) reflection was also observed. This XRD pattern of Mn-SBA-12 is consistent with an ordered, three-dimensional, hexagonal mesoporous structure having $p6_3/mmc$ space group [8]. Mn-SBA-16 (Si/Mn output molar ratio = 278) showed an intense peak at 0.92° [(110) reflection] and two weak peaks at 1.28° and 1.72° [(200) and (211) reflections, respectively] which could be indexed to a three-dimensional, mesoporous, cubic structure with space group of $Im\bar{3}m$ [8]. Except for a weak, broad peak (at ~23°) due to microporous silica, no other peaks due to crystalline manganese oxide phase were detected in the wide-angle region (Fig. 1) revealing that manganese is highly dispersed.

Nitrogen-physisorption isotherms of Mn-SBA-12 were typical of type-IV with H_1 type hysteresis loop corresponding to hexagonal mesopore structure. Mn-SBA-16 showed type-IV isotherms but with a broad H_2 type hysteresis loop revealing that the material has cubic cage-like interconnected mesopore structure (Supplementary data, S2). The specific surface area (S_{BET}) of Mn-SBA-16 decreased (from 800 to 569 m^2/g) with increasing Mn content. Mn-SBA-12 (Si/Mn = 230) has S_{BET} of 587 m^2/g. All these materials showed narrow pore size distribution with its average value in the range of 2.7–3.5 nm. Unit cell parameters and textural properties of these catalysts are listed in Table 1. ICP analysis revealed that only a small portion of input Mn got incorporated into the structure. While a large number of mesoporous solids (M41S type) are prepared in alkaline conditions, SBA materials of this study are prepared in highly acidic conditions. Under such conditions, Mn exists in its cationic form than as oxy/hydroxy species. The former cannot be introduced easily into the framework via condensation processes with silica species in acidic conditions. Moreover, the ionic radius of Mn^{2+} in tetra-coordination is higher (0.066 nm) than that of Si^{4+} (0.026 nm). In view of all these, only a small portion of input Mn got introduced into SBA-12 and SBA-16 lattices. High resolution transmission electron microscopic (HRTEM) images of Mn-SBA-12 and Mn-SBA-16 confirmed long-range, three-dimensional mesoporous ordering of these materials (Fig. 2). The electron diffraction pattern (inset) shows that these materials are crystalline in nature. In conformity with XRD data, no separate bulk manganese oxide-like particles were detected even in HRTEM.

Mn-SBA-12 and Mn-SBA-16 showed four overlapping absorption bands at 215, 270, 345 and 500 nm, respectively (Fig. 3). The bands at 215 and 270 nm are assigned to $O^{2-} \rightarrow Mn^{3+}$ charge-transfer transitions of Mn ions in tetra-coordinated geometry [9]. The band at 345 nm is associated with Mn_3O_4 type species with Mn in hexa-coordinated geometry. A part of Mn is also present in +2 oxidation state which showed crystal field transitions ($^6A_{1g} \rightarrow {}^4T_{2g}$) at 500 nm [9]. As the Mn content increased, the absorption bands have broadened and red shifted. UV–visible spectroscopy, thus, reveals that manganese ions in Mn-SBA-12 and Mn-SBA-16 are present in both +3 and +2 oxidation states in tetrahedral as well as in octahedral coordination geometries.

In general, all these samples are paramagnetic and showed a sextet-line hyperfine pattern in the electron paramagnetic resonance (EPR) spectrum centered at $g_{av} = 2.002$ which is typical for Mn^{2+} ions ($3d^5$, S = 5/2, I = 5/2) in an octahedral environment of oxygen atoms [9–11]. However, intensity of normalized EPR signal increased with increasing Mn content in the catalyst indicating that in catalysts with higher Si/Mn ratio, Mn is mostly in a +3 oxidation state. Increasing amounts of Mn^{2+} species were present as Si/Mn ratio decreased. Mn^{3+} are non-Kramers ions ($3d^4$, S = 2) and they don't show EPR signals at X-band frequency [12]. The EPR signals of Mn^{2+} became

Table 1
Chemical composition and textural properties.

Catalyst	Si/Mn molar ratio		S_{BET} (m^2/g)[b]	Pore volume (cm^3/g)[b]	Average pore size (nm)[b]	Acidity (mmol/g)[c]
	Input	Output[a]				
SBA-16	–	–	800	0.67	3.4	0.04
SBA-12	–	–	672	0.64	3.8	0.03
Mn-SBA-16 (748)	80	748	585	0.50	3.4	0.27
Mn-SBA-16 (736)	50	736	627	0.71	3.4	0.28
Mn-SBA-16 (649)	40	649	569	0.39	2.7	0.29
Mn-SBA-16 (348)	30	348	585	0.45	3.1	0.30
Mn-SBA-16 (278)	20	278	625	0.48	3.1	0.34
Mn-SBA-12 (230)	20	–	587	0.51	3.5	0.39

[a] ICP-OES.
[b] N_2-physisorption.
[c] NH_3-TPD.

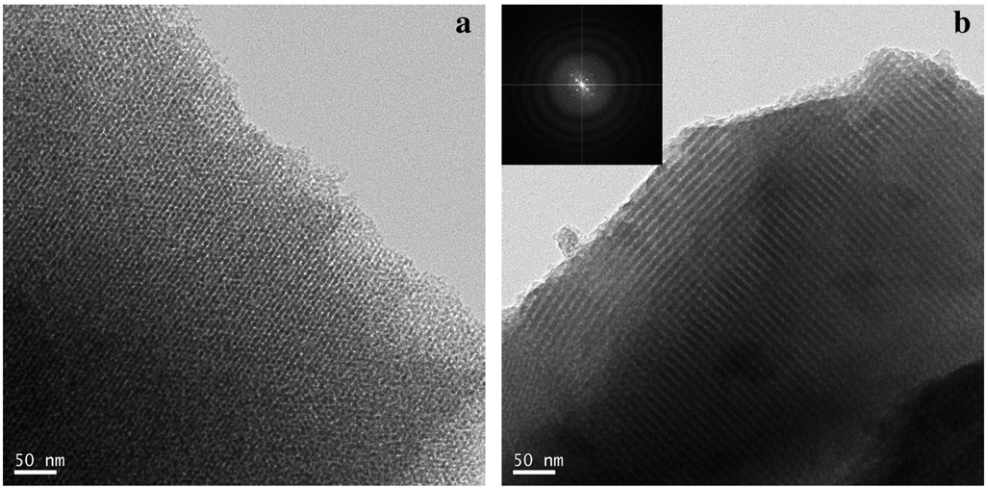

Fig. 2. HRTEM images: (a) Mn-SBA-12 (Si/Mn = 230) and (b) Mn-SBA-16 (Si/Mn = 278).

narrower at 77 K and showed forbidden signals in between the allowed signals (Fig. 4). From the spectral study it can be concluded that the framework substituted Mn is in a +3 oxidation state and the extra framework Mn is in a +2 state.

Temperature-programmed desorption of ammonia (NH_3-TPD) studies determining acidity of the catalysts showed three desorption peaks with maximum at 456, 600 and 645 K (Supplementary data, S3). While the first peak is attributed to ammonia desorbed from weakly acidic silanol groups, the latter two are attributed to desorptions from strong acidic sites (framework-substituted, tetrahedral manganese ions). The overall acidity of Mn-SBA-12 was higher (0.39 mmol/g) than that of Mn-SBA-16 (0.26–0.34 mmol/g) (Table 1). This agrees well with the higher Mn content in Mn-SBA-12 than in Mn-SBA-16.

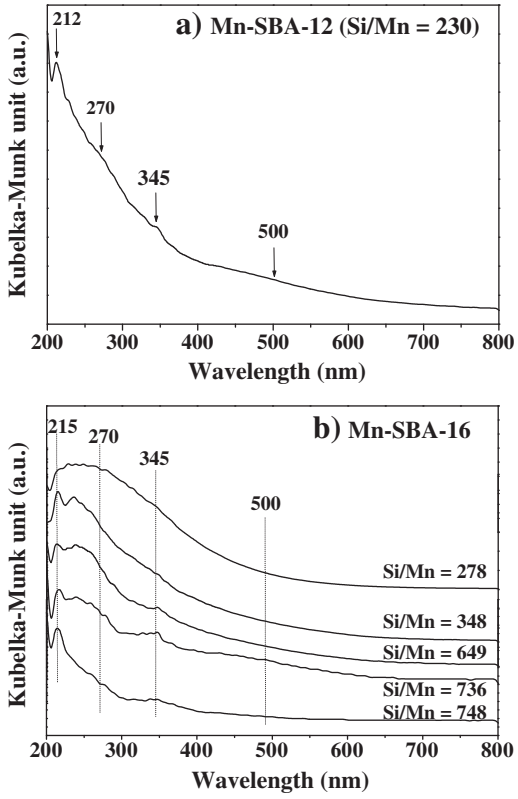

Fig. 3. Diffuse reflectance UV–visible spectra.

3.2. Catalytic activity

Benzylamine (A) can be converted directly into benzamide (B) by simultaneously reacting with air and aqueous ammonia in presence of a catalyst. 1,4-Dioxane was the suitable solvent because of high solubility of A, ammonia and water in it. Benzamide (B), benzylidinebenzylamine (C), benzaldehyde (D) and benzonitrile (E) are possible oxidation products in this reaction. Product E was not detected while using Mn-SBA-12 and Mn-SBA-16. However, a small amount of unidentified products (others) was observed at certain reaction conditions. Blank, controlled experiments revealed that the reaction of A doesn't take place in the absence of catalyst. Bulk MnO_2 was active and 100 mol% conversion of A was observed but benzamide selectivity was significantly low (4.7 mol%). Turnover frequency (TOF) of MnO_2 was very low ($<1\ h^{-1}$). Both Mn-SBA-12 and Mn-SBA-16 showed high catalytic oxidation activity (conversion of A = 100 mol%) (Table 2). Mn-SBA-16 (Si/Mn output molar ratio = 736) showed higher selectivity for benzamide (40.3 mol%). TOF and benzamide yield increased with decreasing Si/Mn ratio up to a value of 736 and thereafter, showed a decreasing trend revealing that only the framework substituted Mn in +3 oxidation state are more active and product B selective while the extra framework Mn^{2+} preponderant in low Si/Mn catalysts are selective for product C. Neat SBA-12 and SBA-16 were also active but conversion of A was 70 mol% and benzamide selectivity was 20 mol% only,

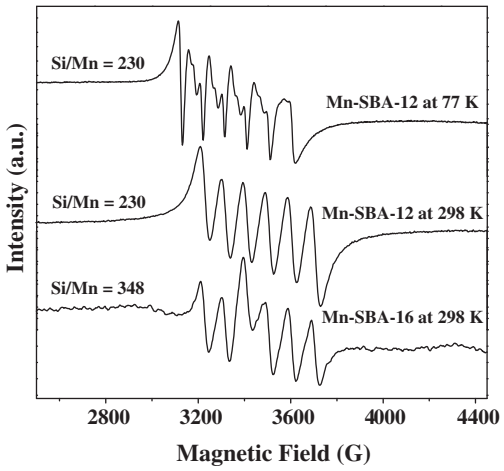

Fig. 4. EPR spectra of Mn-SBA-12 and Mn-SBA-16.

Table 2
Catalytic activity of Mn-SBA-12 and Mn-SBA-16.[a]

Catalyst	TOF (h^{-1})	Product yield (mol%)			
		B	C	D	Others
MnO_2	<1	4.7	95.3	0	–
Mn-SBA-16 (748)	103	36.0	46.9	11.6	5.5
Mn-SBA-16 (736)	138	40.3	44.7	15.0	–
Mn-SBA-16 (649)	122	34.0	51.1	14.9	–
Mn-SBA-16 (348)	65	19.3	78.0	1.7	–
Mn-SBA-16 (278)	43	25.6	68.9	6.4	–
Mn-SBA-12 (230)	52	30.9	62.3	6.8	–
Mn–Al-SBA-16 (350)	–	24.5	54.3	9.7	11.5

[a] Reaction conditions: Catalyst = 0.2 g, benzylamine (A) = 5 mmol, aqueous NH_3 (25%) = 1 mL, 1,4 dioxane = 15 mL, air = 6 bar, reaction temperature = 423 K and reaction time = 8 h. Turn over frequency (TOF) = moles of benzylamine converted per mole of Mn (output) in the catalyst per hour. Conversion of A = 100 mol%. B = benzamide, C = benzylidinebenzylamine and D = benzaldehyde.

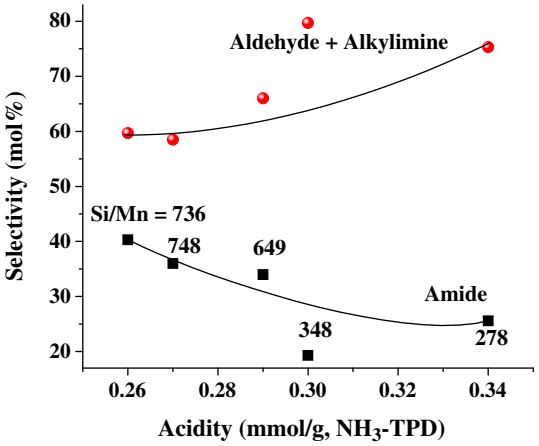

Fig. 5. Acidity verses product selectivity correlation over Mn-SBA-16.

Table 3
Influence of reaction temperature on the conversion of benzylamine to benzamide[a].

Run no.	Reaction temperature (K)	Conversion of A (mol%)	TOF (h^{-1})	Product selectivity (mol%)		
				B	C	D
1	373	10.2	14	–	100.0	–
2	403	90.0	124	26.2	73.8	–
3	423	100.0	138	40.3	44.7	15.0

[a] Reaction conditions: Catalyst, Mn-SBA-16 (Si/Mn = 736) = 0.2 g, benzylamine (A) = 5 mmol (0.53 g), aqueous NH_3 (25%) = 1 mL, solvent = 1,4 dioxane (15 mL), stirring speed (rpm) = 600, reaction pressure = 6 atm and reaction time = 8 h. TOF (turn over frequency) = number of moles of benzylamine converted per mole of Mn (output) present in the catalyst per hour. B = benzamide, C = benzylidinebenzylamine and D = benzaldehyde.

suggesting that framework substituted Mn enhances the catalytic activity and benzamide selectivity.

Temperature and pressure showed notable effects on conversion of A and product B selectivity (Table 3; Supplementary data, S4). When the reaction was performed at 373 K over Mn-SBA-16 (Si/Mn = 736), conversion of A was 10.2 mol% and C was the only product. As the temperature was increased to 403 K, conversion of A increased to 90 mol% and selectivities for B and C were 14.5 and 73.8 mol%, respectively. At 423 K, complete conversion of A was observed and amide formed with a selectivity of 40.3 mol% (Table 3). When the reaction was continued for 10 h, selectivity of B increased to 47.1 mol% (Supplementary data, S4). Also an increase in product B selectivity was observed when pressure was raised from 6 to 10 bar. Incorporation of Al^{3+} in the catalyst led to reduced selectivity of benzamide.

In this reaction, amine (A) is converted into an intermediate aldimine through oxidative dehydrogenation (Scheme 1) which undergoes further transformation by two pathways [7]. Oxidative dehydrogenation which is dependent on metal redox behavior and hydrolysis/amination which are dependent on acidic character of the catalyst are the two competing reactions controlling product selectivity. Complete conversion of A indicates that the first step (amine to aldimine) is facile. Acidity verses redox property of the catalyst determines whether aldimine undergoes hydrolysis to benzaldehyde (D) which further reacts with A to form benzylidinebenzylamine (C) or follows the other route. The backward reaction of benzaldehyde (D) to aldimine can also take place in presence of ammonia. But, benzylamine is more basic than ammonia [pK_b = 4.66 (benzylamine) and 4.75 (ammonia)] and hence, formation of C is preferred over acid catalysts to the reverse reaction of D to aldimine. Moreover, aldimine could not be detected suggesting that it is an intermediate at our experimental conditions. Under mild acidic conditions and Mn with a facile redox state, further oxidative dehydrogenation followed by hydrolysis and amination converts aldimine into benzamide (B). Benzaldehyde (D) can get further oxidized to benzoic acid which upon reaction with ammonia forms a salt that can settle on the catalyst. Analysis of the spent catalyst by FTIR spectroscopy ruled out that possibility at our experimental conditions (Supplementary data, S5).

As seen from Fig. 5, with increasing acidity of the catalyst higher amounts of (C + D) have formed and the selectivity for B decreased. As noted before with decreasing Si/Mn ratio, the concentration of Mn^{2+} (electronic band at 500 nm and sextet-line EPR pattern) has increased. At higher Si/Mn ratio, most of the Mn is in +3 oxidation state. While both the Mn species are active for the conversion of A to aldimine, only Mn^{3+} facilitate amide formation while the extra framework Mn^{2+} lead to (C + D). Thus, weak acidity and framework substituted Mn^{3+} ions are the key features responsible for the high catalytic activity of Mn-SBA-16 and Mn-SBA-12 in the direct oxidation of primary amines to amides.

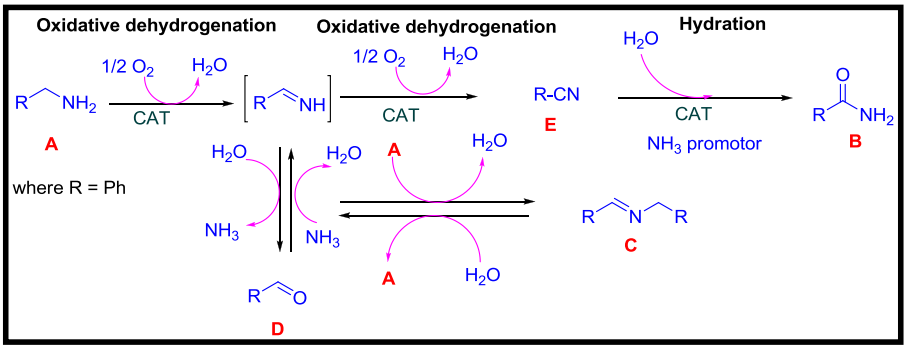

Scheme 1. Reaction mechanism for formation of amides from primary amines.

4. Conclusions

Catalytic application of Mn-SBA-12 and Mn-SBA-16 for the eco-friendly synthesis of amide from primary amine (benzyl amine, for example) was reported. The catalysts contained manganese in +2 and +3 oxidation states, concentration of the former increased with decreasing Si/Mn ratio. Both acidity and oxidation state of Mn controlled amide selectivity in the product.

Acknowledgment

AK and DN acknowledge Council of Scientific and Industrial Research (CSIR), New Delhi for the Research Fellowship.

Appendix A. Supplementary data

Supplementary data to this article can be found online at http://dx.doi.org/10.1016/j.catcom.2013.03.020.

References

[1] U.S. Patent 5,626,836 (1997).
[2] E. Valeur, M. Bradley, Chemical Society Reviews 38 (2009) 606–631.
[3] M.B. Smith, J. March, Advanced Organic Chemistry: Reactions, Mechanisms, and Structure, 6th ed. Wiley, Hoboken, NJ, 2007.
[4] C. Gunanathan, Y.B. David, D. Milstein, Science 317 (2007) 790–792.
[5] H. Fujiwara, Y. Ogasawara, K. Yamaguchi, N. Mizuno, Angewandte Chemie International Edition 46 (2007) 5202–5205.
[6] J.W. Kim, K. Yamaguchi, N. Mizuno, Angewandte Chemie International Edition 47 (2008) 9249–9251.
[7] Y. Wang, H. Kobayashi, K. Yamaguchi, N. Mizuno, Chemical Communications 48 (2012) 2642–2644.
[8] D. Zhao, Q. Huo, J. Feng, B.F. Chmelka, G.D. Stucky, Journal of the American Chemical Society 120 (1998) 6024–6036.
[9] K.M. Parida, S.S. Das, Journal of Molecular Catalysis A: Chemical 306 (2009) 54–61.
[10] M. Selvaraj, T.G. Lee, The Journal of Physical Chemistry B 110 (2006) 21793–21802.
[11] A. Ramanathan, T. Archipov, R. Maheswari, U. Henefeld, E. Roduner, R. Gläser, Journal of Physical Chemistry Part C 112 (2008) 7468–7476.
[12] D.P. Goldberg, J. Telser, J. Krzystek, A.G. Montalban, L.-C. Brunel, A.G.M. Barrett, B.M. Hoffman, Journal of the American Chemical Society 119 (1997) 8722–8723.